Electronic Supplementary Material (ESI) for Chemical Communications
This journal is © The Royal Society of Chemistry 2013

Sequential formation of N-doped nanohelicene, nanographene and nanodome by surface-assisted chemical (cyclo)dehydrogenation of heteroaromatics.

Supplementary Information

Anna Lisa Pinardi,[1] José Ignacio Martínez,[1] Andrej Jančařík,[2] Irena G Stará,[2] Ivo Starý,[2] Maria Francisca Lopez,[1] Javier Mendez,[1] Jose Angel Martin-Gago[1, 3]

1 Instituto de Ciencia de Materiales de Madrid ((ICMM),Consejo Superior de Investigaciones Científicas (CSIC), Sor Juana Inés de la Cruz 3,, Cantoblanco, 28049 Madrid, Spain

2 Institute of Organic Chemistry and Biochemistry, Academy of Sciences of the Czech Republic, Flemingovo nám. 2, 166 10 Prague 6, Czech Republic

3 Centro de Astrobiología (CSIC-INTA), Carretera de Torrejón a Ajalvir, km 4, 28850 Torrejón de Ardoz, Madrid, Spain

* José A. Martin-Gago: gago@icmm.csic.es

1. SYNTHESIS OF PYRIDYL-DISUBSTITUTED DIBENZO[5]HELICENE

The chemical synthesis of pyridyl disubstituted dibenzo[5]helicene **1** (DiPy[5]DBH) has been described in detail elsewhere.[1] Owing to its helical arrangement, the compound **1** exists in the form of (*M*) and (*P*) enantiomers. In this study, a racemic mixture of **1** was used.

2. EXPERIMENTAL DETAILS

The experiments were carried out in a UHV chamber with base pressure of $1x10^{-10}$ mbar. The Pt(111) sample was cleaned by sputtering in Ar^+ atmosphere (10 μA) followed by annealing cycles to 1200 K. Due to the high reactivity of the sample, annealing cycles in O_2 atmosphere (1200 K in 2×10^{-6} mbar of O_2) were necessary to get rid of some contaminations.

The molecules were evaporated at a rate of 0.1 ML/min at 575 K from a homemade Ta crucible whose temperature was controlled by a type-K thermocouple, and during the deposition the pressure never exceeded 5×10^{-10} mbar.

The STM images were recorded in constant current mode with typical tunnelling current values of 0.2 nA and sample voltage of 2.0 V.

3. COMPUTATIONAL DETAILS

3.1 General aspects

For ab-initio atomistic simulations of the different adsorbate/Pt(111) configurations analysed in this study (ranging from the pristine molecule **1** to the N-doped nanodome **4** as adsorbates), Density Functional Theory was used effectively combining the localised-basis-set and plane-wave schemes as implemented in the Fireball[2] and PwScf[3] simulation packages, respectively. All the calculations include van der Waals corrections in a perturbative framework, widely described elsewhere (ref. [4] and references therein). The exchange-correlation effects have been accounted by using the local density PW91 parametrisation,[5] and norm-conserving scalar-relativistic pseudopotentials[6] have been considered to model the ion-electron interaction. The Pt(111) surface was modelled in a repeated slab geometry: a slab of four Pt(111) layers with a distance of ~ 25 Å of vacuum between neighbouring cells along the axis perpendicular to the surface was used as well as full periodic boundary conditions representing an infinite Pt(111) surface. Each substrate layer contained 100 Pt atoms and the size of the unit cell in the direction parallel to the surface was 28.1 × 28.1 $Å^2$, large enough to avoid any possible intermolecular interaction between neighbouring cells. To define the equilibrium properties of the different structural configurations involved along the (cyclo)dehydrogenation process, we carried out full geometry optimisations, and only the two bottom Pt layers were kept fixed.

3.2 Theoretical STM imaging

In our STM approach, tunnelling currents for the STM images have been calculated using a Keldysh–Green function formalism, together with the first-principles tight-binding Hamiltonian obtained from the local-orbital DFT-Fireball method (as explained in detail elsewhere[2,7,8]). Some examples of the application of this approach can be found in refs [9–11] and, in particular, ref. [9] is a good example of how the accurate theoretical simulation of STM images, and its comparison with high-quality experimental STM images, can guide us towards the correct atomic structure of an organic molecule on a metal substrate. Within this formalism, the tip (a

standard pyramidal clean W-tip in our case) and the sample (adsorbate/Pt(111)) are calculated independently providing independent subsystem Hamiltonians. Thus, the overlapping Hamiltonian is obtained by using a dimer approximation: a dimer formed by one W atom (corresponding to the tip) and another one (H, C, N or Pt coming from the sample) is calculated for different atom–atom distances and for all the non-zero interactions, using the Keldish-Green formalism to propagate the tunnel current between both subsystems. The details are widely explained by Blanco et al. in refs. 7 and 8 (and references cited therein). The theoretical STM images have been obtained at constant-current scanning conditions, moving the W-tip perpendicularly to the sample in each scanning stage to search a pre-selected fix value of the tunnel current. The theoretical scanning parameters used here were I_{tunnel} = 0.2 nA, and $V_{substrate}$ = +2 V, in order to mimic the experimental procedure. Given the electrostatic nature of this interaction, the influence of the Pt(111) substrate on the theoretical STM images will not be important, since, in first approximation, the electronic structure of the molecules will remain almost unaltered.

4.- NANODOME FORMATION

One of the most relevant discoveries of the present communication is the direct observation of the formation of fully dehydrogenated domes from nanographenes after annealing above 770 K. Fig. S1 shows the side view and the top view of four different steps of the DFT-based molecular dynamics process for the fully dehydrogenation of the molecule on Pt(111). The whole molecular dynamics movie has been submitted as additional material. Once **3** completes the temperature-assisted dehydrogenation, the peripheral dangling bonds of the nanographene **3** tend to bind covalently to the surface. The molecule bends in such a way that becomes a distorted dome covalently adsorbed to the Pt(111) surface. We speculate that a molecular design with a pentagon in the middle, as the proposed by Amsharov et al. could lead to the formation of nanotube-cup.[12] The preferential adsorption sites of the dangling bonds of the edge C atoms on the Pt(111) surface is “on top” of the Pt atoms. For this to occur, the whole molecule needs to resize the parallel effective area by pulling up the central part of the molecule, in order for all the edge C atoms to covalently attach to the Pt atoms underneath at an average distance around 2.3 Å. Hence the final configuration results in a semi-spherical bent N-doped coronene. On the other hand, DFT calculations predict an adsorption energy for this bent dome on Pt(111) of around 2.9 eV below that corresponding to the precursor **1**, to be

compared with those adsorption energies corresponding to the **2** and **3** intermediates of around 1.8 and 2.5 eV, respectively (see [1])

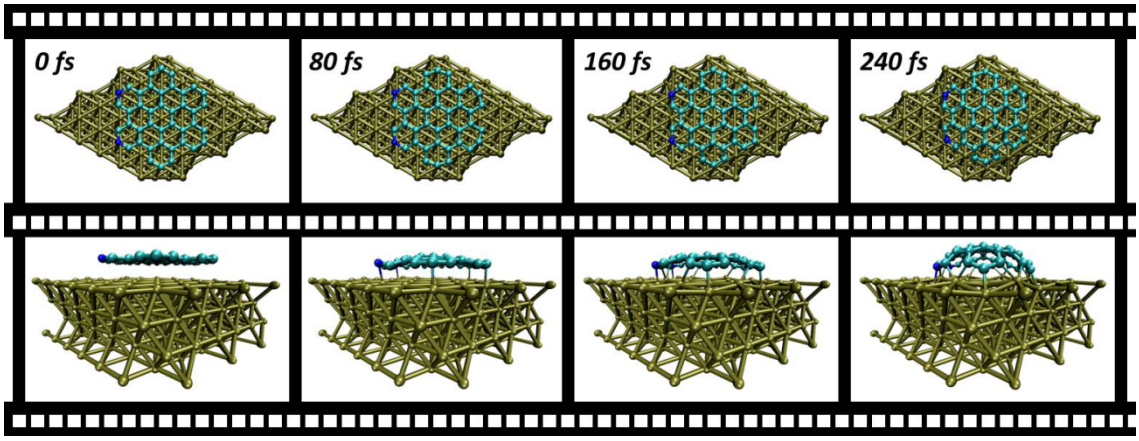

Fig. S1 – Top (top row) and side (bottom row) views of four different steps (for t^{MD}=0, 80, 160 and 240 fs) along the molecular dynamics process at 800K once the molecule reaches full dehydrogenation.

5.- ADDITIONAL STM IMAGES AND ANALYSIS

Fig. S2a-d and Fig. S2e-f represent 25 × 25 nm^2 and 7 × 7 nm^2 STM images of all the four dehydrogenation stages described in the article. The structural transformation is clear in each stage. At 300 K the molecules reveal the four-lobe structure confirming that they are intact (the DiPy[5]DBH precursor **1**): Fig. S2e shows molecular orbital resolution of four molecules.

Annealing to 450 K (Fig. S2-b, f) shows the structural transformation of **1** into **2**, caused by the cleavage of six C-H bonds and the consequent cyclodehydrogenation. In the zoom we can see that the molecules orient in different ways and one side of them (corresponding to that one of the pyridine rings) is higher than the other. By being able to image these molecules we confirm that this cyclodehydrogenation stage is stable and can be isolated.

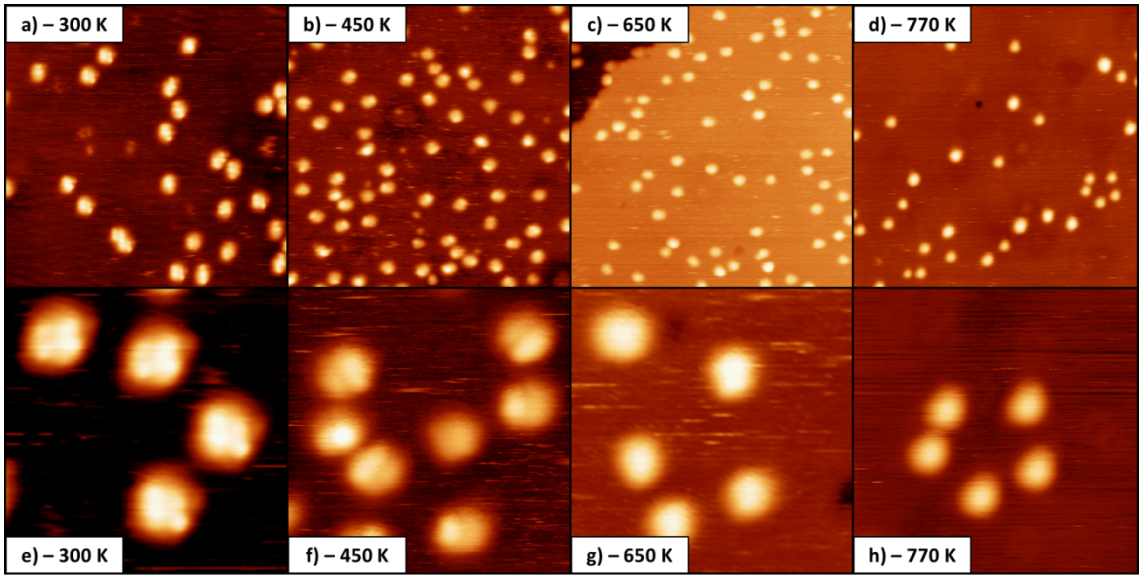

Fig. S2 – (a-d) 25 × 25 nm^2 STM images of the precursor DiPy[5]DBH **1**/Pt(111) at different annealing temperatures (V_{sample} = 2.0 V): 300 K (**1**), 450 K (**2**), 650 K (**3**) and 770 K (**4**). (e-h) 7 × 7 nm^2 high resolution images of each stage (V_{sample} = 2.0 V).

When annealing at 650 K (Fig. S2-c, g), all molecules are very similar: the cyclodehydrogenation completes and diazahexabenzocoronene (2N-HBC), namely N-doped nanographene flakes **3** are formed. At this stage, the H atoms are still present at the edge of the molecules, but when annealing at 770 K (Fig. S2d, h) dehydrogenation of the molecule is complete and N-doped nanodomes **4** arise.

To statistically understand the efficiency of the stepwise formation of molecules **3** and **4**, we developed a histogram which reveals the percentage of type-**3** and type-**4** molecules at 650 K (majority of nanographenes **3**) and at 770 K (majority of nanodomes **4**), which is shown in Fig. S3. As the apparent heights of **3** and **4** are quite different, we can differentiate their relative percentage by counting how many molecules existed with an apparent height higher than 0.22 up to 0.28 nm (type-**3**) and between 018-0.22 nm (type-**4**) at each temperature.

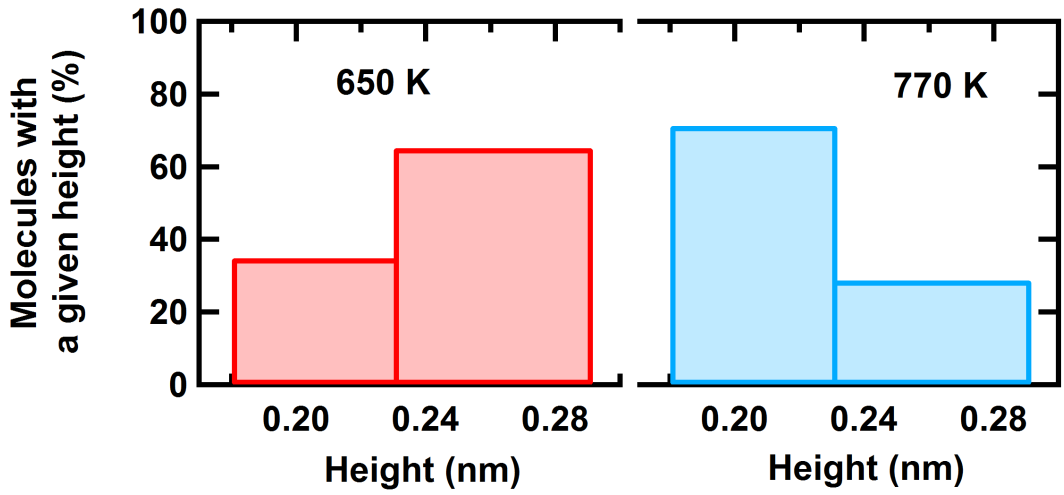

Fig. S3 – Histogram of the apparent height of molecules at 650 K (red) and at 770 K (blue). Type-**3** molecules (nanographenes) are considered to exhibit an apparent height higher than 0.22 nm up to 0.28 nm, and type-**4** molecules (nanodomes) to have an apparent height between 0.18 and 0.22 nm. According to the histogram, at 650 K, 65.2 % of molecules are nanographenes; at 770 K, 71.2 % of molecules are nanodomes.

For the histogram to be statistically relevant we recorded the apparent height of 85 (75) molecules for images at 650 K (770 K). At 650 K, 65.2 % of molecules are nanographenes, and at 770 K 71.2 % of molecules are nanodomes. Hence, the dehydrogenation of **3** into **4** is a slow process, as the two stages coexist for a wide range of temperatures. Nevertheless, the STM images and this histogram clearly indicate the tendency of the edge H-atoms to detach and allow the formation of bent nanodomes covalently bonded to the metal surface.

Fig. S4 shows the experimental (left) and theoretical (right) apparent height of 2N-HBC **3** in red compared to that one of the N-dome **4** in blue. Although **3** is planar, its apparent height is higher than that of the curved dome **4**. In fact, the H atoms at the edge of **3** passivate the border C atoms, hence preventing covalent interaction with the Pt. The absence of the peripheral H atoms in **4** allows for the covalent bonding between **4** and the metal, which brings them closer and lowers the apparent height of **4** with respect to **3**.

From Fig. S3 we can see that at this temperature not all of the molecules transform into nanodomes, but about 28% of them are still larger and taller than the nanodome that indicates the presence of nanographenes even at this temperature.

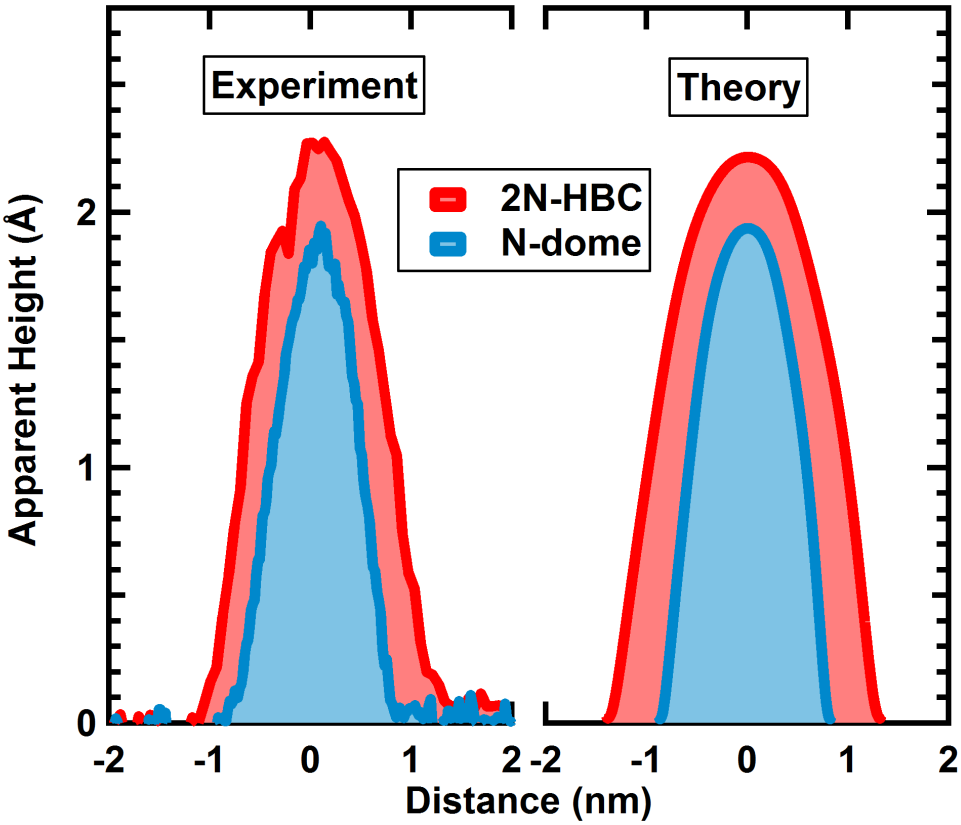

Fig. S4 – The apparent height of **3** (2N-HBC) in red is compared to that one of **4** (N-dome) in blue. The nanodome is smaller than the nanographene both in height and width. The experimental (left) and the theoretical (right) apparent heights are both qualitatively and quantitatively similar.

6. N-DOPPED GRAPHENE

As discussed in the text, upon annealing the molecules decompose into graphene. It is well known[13] that the use of large polycyclic aromatic hydrocarbons and of low annealing temperatures favour the growth of small islands of different domains of graphene on Pt(111). We have been observing a similar tendency. When annealing above 900 K, the molecules decompose into graphene. Fig. S5 shows two 35x35 nm^2 images of graphene grown by annealing **1** at 900 K. Fig. S5-a represents a low coverage sample (room temperature deposition), where only a few sporadic islands of graphene are present: the low coverage of the precursor does not allow to completely covering the Pt surface. Fig. S5-b on the other hand represents a sample on which about two monolayers of **1** were deposited on the Pt surface kept at 900 K. The large amount of material and the relatively low annealing temperature used favours the formation of small domains with a different angle with respect to the surface. The

Greek letters represent the different superstructures according to the nomenclature presented in ref. 13 These domains are surrounded by undecomposed carbonaceous chains of molecule, which are still present due to the low annealing temperature, which is not enough to decompose all the molecules into graphene.

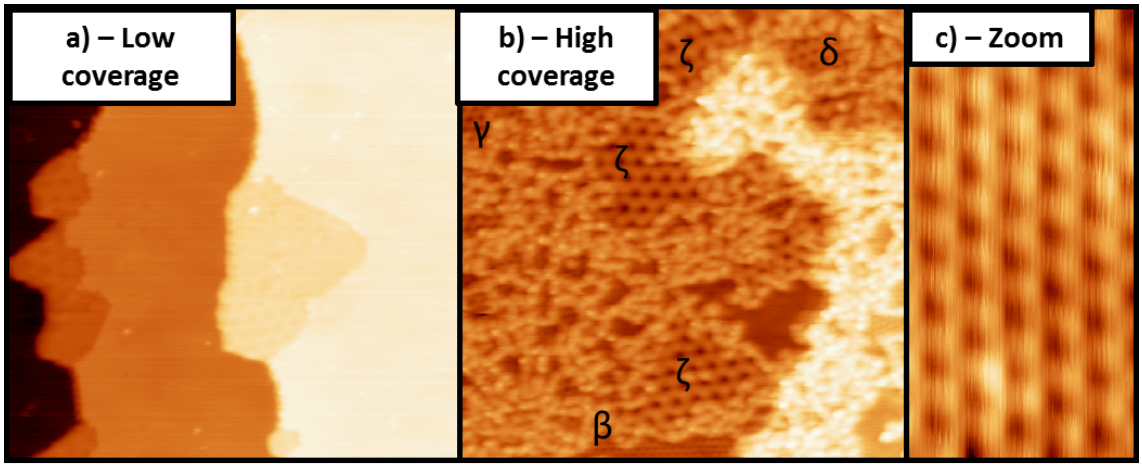

Fig. S5 – 35x35 nm^2 graphene images grown by annealing **1**. a) Low coverage of **1** annealed at 900 K favours the growth of small islands of different domains of graphene close to the steps (V_{sample} = 0.3 V). b) When about two monolayers of **1** are deposited on the surface kept at 900 K, small islands of graphene surrounded by undecomposed chains of molecules are observed (V_{sample} = 0.01 V); the Greek letters represent the different domains according to the nomenclature presented in ref.[12]

7 ADDITIONAL REFERENCES

1. A. L. Pinardi, G. Otero-Irurueta, I. Palacio, J. I. Martinez, C. Sanchez-Sanchez, M. Tello, C. Rogero, A. Cossaro, A. Preobrajenski, M. F. Lopez, J. Méndez, A. Jancarik, I. G. Stara, I. Stary, and J. A. Martin-Gago, *ACS Nano*, 2013, **7**, 3676–3684.

2. J. P. Lewis, P. Jelínek, J. Ortega, A. A. Demkov, D. G. Trabada, B. Haycock, H. Wang, G. Adams, J. K. Tomfohr, E. Abad, H. Wang, and D. A. Drabold, *Physica Status Solidi B*, 2011, **248**, 1989–2007.

3. S. Baroni, A. D. Corso, S. De Gironcoli, and P. Giannozzi, 2005.

4. Y. J. Dappe and J. I. Martínez, *Carbon*, 2013, **54**, 113–123.

5. J. P. Perdew, K. A. Jackson, M. R. Pederson, D. J. Singh, and C. Fiolhais, *Physical Review B*, 1992, **46**, 6671–6687.

6. D. Vanderbilt, *Physical Review B*, 1986, **41**, 7892–7895.

7. J. M. Blanco, C. González, P. Jelínek, J. Ortega, F. Flores, and R. Pérez, *Physical Review B*, 2004, **70-78**.

8. J. M. Blanco, F. Flores, and R. Pérez, *Prog. Surf. Sci.*, 2006, **81**, 403–444.

9. J. I. Martínez, E. Abad, C. González, J. Ortega, and F. Flores, *Physical Review Letters*, 2012, **108**, 246102.

10. J. I. Martínez, E. Abad, F. Flores, and J. Ortega, *Physica Status Solidi (B)*, 2011, **248**, 2044–2049.

11. E. Abad, Y. J. Dappe, J. I. Martínez, F. Flores, and J. Ortega, *The Journal of chemical physics*, 2011, **134**, 044701.

12. Mueller, A. and Amsharov, K. Yu. (2012),. Eur. J. Org. Chem., 2012: 6155–6164.

13. P. Merino, M. Svec, A. L. Pinardi, and G. Otero, *ACS Nano*, 2011, **5**, 5627–5634.